PROCEEDINGS, 50th Workshop on Geothermal Reservoir Engineering
Stanford University, Stanford, California, February 10-12, 2025
SGP-TR-229

Small Unoccupied Aerial Systems (UAS) and Thermal Cameras in Geothermal Exploration and Operational Fields; a Review of UAS Equipment and Case Study at Brady Geothermal Field, Nevada USA

Courtney Brailo, Madeline Churchill, Tiara Bechtold, Kelly Blake and Robin Zuza

Ormat Technologies, Inc., 6884 Sierra Center Parkway, Reno NV, 89511

cbrailo@ormat.com

Keywords: UAS, drone, thermal, imagery, geothermal, exploration, operations, remote sensing, Ormat, North America, Nevada, Basin and Range, Great Basin, springs, surface manifestations

ABSTRACT

Unoccupied Aerial Systems (UAS, drones) are increasingly utilized in geologic and geothermal analysis, commonly used for collection of high-resolution aerial imagery and associated products (e.g., orthorectified photomosaics, digital surface models). Recent advancements in UAS technology, portability, GPS accuracy, price, and diversity of attachments (payloads) have occurred alongside improvements in digital image reconstructions and scope of Federal Aviation Administration regulations, making drones more applicable to geothermal operations. Small UAS are easy to transport and deploy but have limiting factors such as fixed payloads and reduced flight ranges. Larger UAS increase flight efficiency and are capable of interchangeable payload systems, but are significantly more expensive and require additional resources to mobilize equipment. Thermal camera payloads, originally intended to aid in search-and-rescue efforts, are now being deployed in geothermal fields to refine surface temperature maps, in both exploration and operational phases of geothermal research. In February of 2024, daytime conventional and nighttime thermal imagery was collected at the Brady geothermal field in Nevada, USA. Brady is an operational field in the Basin and Range that has been producing power since 1992. The survey imaged plant operational infrastructure and geologic features, including uninsulated pipelines and surface manifestations, at a higher detail than previously possible. These data help support plant operations and troubleshooting, and increase accuracy of geologic mapping of the field. This study reviews UAS equipment, summarizes historic technological advances, and highlights the work completed at Brady. This work serves as a test case for further deployment of UAS across Ormat's operational and exploration fields to improve field work safety, efficiency, and thorough data collection.

1. INTRODUCTION

Geothermal resources are a key baseload contributor to renewable power generation; however, these resources require significant amounts of research and exploration to identify, investment in development and construction of facilities, and regular infrastucture system control and maintenance when in operation. Technological advancements are continually being evaluated across the geothermal industry to drive down costs and increase exploration and operational success and efficiency; Unoccupied Aerial Systems (UAS, drones) developments are becoming a valuable tool in supporting this work. Recent advancements of UAS technology have improved safety, efficiency, and effectiveness of daily work across many industries (Gheisari and Esmaeili, 2016; McGuire et al., 2016; Hubbard et al., 2017; Aminifar and Rahmatian, 2020). In this study we explore the utility of thermal UAS for geothermal operational support to map infrastructure and surface manifestations using high-quality UAS data collection. We highlight how improvements across many technologies and methodologies make these studies possible.

Infrastructure and reservoir management play a critical role in maintaining generation capacity at geothermal fields, UAS operations can now be used to create 3D models of facilities, conduct transmission inspections, and support construction operations (Canis, 2015; Aminifar and Rahmatian, 2020). Across the Energy industry, drones have increasingly been used for inspection of infrastructure, like powerlines and poles, with an emphasis on empowering and protecting the workforce (Aminifar and Rahmatian, 2020). These surveys allow fieldworkers to inspect equipment, locate issues, and avoid hazards by keeping crews away from dangerous features like high-voltage lines and structures (Rymer and Moore, 2021). UAS surveys also compliment geologic studies by providing current imagery data that may be unavailable in the public domain, especially at a high resolution (Remondina et al., 2011; Whitehead and Hugenholtz, 2014). Imagery collected from UAS equipped with traditional visible light (RGB) cameras have been used in structure-from-motion reconstructions for many years (Wright, 1954; Remondina et al., 2011; Whitehead and Hugenholtz, 2014; Carrivick et al., 2016; Aminifar and Rahmatian, 2020; Jimenez-Jimenez, 2021). This technology, called photogrammetry, takes a multitude of photos and compiles them into detailed orthomosaics, digital terrain, and digital surface models. These imagery data and surface models can be used to improve geologic lithologic and fault maps (Angster et al., 2016; Carrivick et al., 2016; Callahan et al., 2023) that ultimately support exploration and development of geothermal resources.

Improvements of available UAS sensors (e.g., visible, infrared, multispectral) has increased the popularity of UAS. While UAS-mounted thermal infrared (TIR) cameras have been tested and adopted across many industries, including search and rescue (Levin et al., 2016; Yeom, S., 2024), applying photogrammetry to these images, often collected at night, present unique challenges (Burdziakowski and Bobkowska, 2021). For example, during early tests of this technology at Ormat Technologies, Inc. (Ormat), thermally heated surfaces from sunlight created an artificial heat signature that made temperature anomalies difficult to identify, similar to complications identified by previous studies (Coolbaugh et al., 2007). Changes in Federal Aviation Administration (FAA), the regulatory agency for UAS flights

in the United States, allowing nighttime operations for licensed drone operators, along with experimental studies, improved sensors, and processing techniques (Maset et al., 2017), have now increased the overall success of these UAS thermal surveys. These flights are now becoming a successful method for visualizing thermal anomalies in high resolution, especially useful in geothermal applications (Nishar et al., 2015; Harvey et al., 2016; Chio and Lin, 2017; Lai et al., 2018; Bjornsson et al., 2019).

The Brady geothermal field was chosen as a target to test thermal drone capabilities because of its infrastructure (e.g. wells and pipelines), extensive thermal surface manifestations previously mapped in detail (Coolbaugh et al., 2004; Faulds et al., 2010a), relatively cold and dry nights in winter seasons that are useful in thermal UAS surveys, and is conveniently located 50 miles from Ormat's corporate headquarters in Reno, NV (Fig. 1). Coolbaugh et al. (2004) studied thermal imagery and warm ground at Brady using GPS and thermal ground measurements, and satellite thermal and hyperspectral (ASTER) data, and so provides a valuable baseline comparison to data collected in this study.

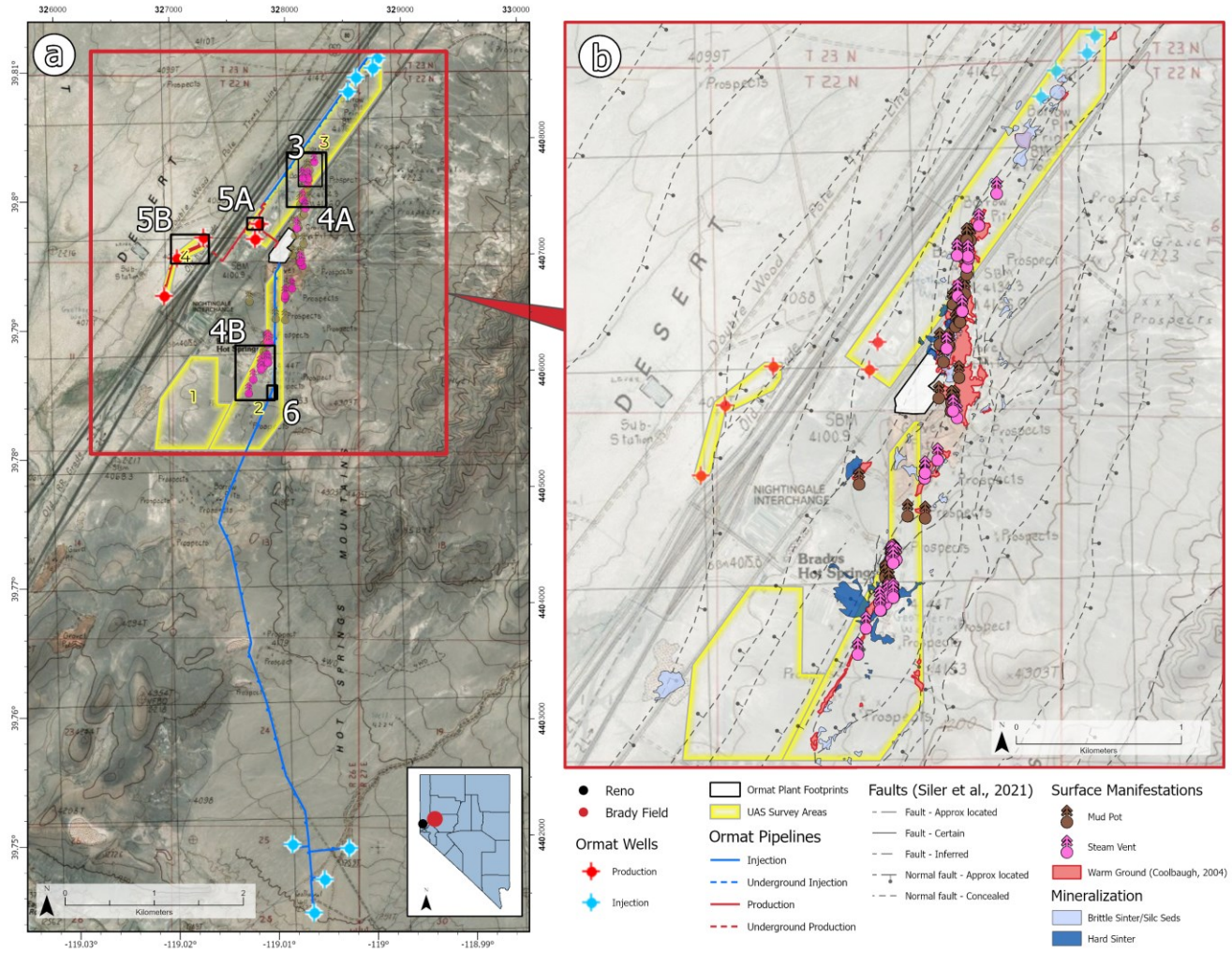

Figure 1: a.) Map of Brady geothermal field, showing plant, pipeline and well locations. Black rectangles correspond with map footprints in figures below, yellow rectangles represent UAS survey areas. b.) Surface manifestations, mineralization, and extent of warm ground and fault zone shown in inset (Coolbaugh et al., 2004; Faulds et al., 2010a, Siler et al., 2021).

2. BACKGROUND

2.1 Brady Geothermal Field

The Brady geothermal field is located 50 miles east-northeast of Reno, along the Hot Springs Mountains in Churchill County, Nevada. Commercial operations began at Brady in 1992, and the field has been operated by Ormat since 2001. The geothermal field is situated within the Great Basin, an area of overlapping Basin and Range extensional and Walker Lane transtensional regimes, with a general extension direction of WNW in this location (Wesnousky et al., 2005, Faulds et al., 2010b).

Brady has been the subject of geothermal exploration since 1959 and has a well-defined structural model and detailed mapping of surface thermal manifestations that include mud pots, steam vents, and warm and steaming ground (Benoit and Butler, 1983; Coolbaugh et al., 2004; Faulds et al., 2010a; Faulds et al., 2010b; Siler et al., 2016). Geothermal upflow is localized along a 1-km wide, 4-km long left

stepover in the NNE-striking, NNW-dipping Brady fault zone (Faulds et al., 2006; Faulds et al., 2010b; Folsom et al., 2018). This fault zone is oriented orthogonal to the regional west-northwest extension direction and is thus favorably oriented for fluid flow (Faulds et al., 2006). Laboso and Davatzes (2016) suggest that complexities in this fault zone, especially areas of high fracture densities, provide the necessary permeability to host the commercial geothermal system found here, and the production wells at the field are located within the main stepover of the Brady fault. Injection is primarily proximal to production, north along strike of the Brady fault, with minor distal injection south of the production area (Fig. 1).

Previous work at the field includes detailed mapping of thermal manifestations by ground-based investigations using hand-held GPS units and personal computers, which identify approximately 300 thermal features (Coolbaugh et al., 2004). Satellite-based ASTER data were also used to image the 4-km long thermal anomaly within the stepover at 90-meter resolution, but these data could not be used to distinguish the individual thermal features (Calvin et al., 2005; Coolbaugh et al., 2007). These studies highlight difficulties using TIR imagery for geothermal modeling and detection of surface temperature anomalies, as variable mineral properties of surface deposits, diurnal solar heating effects, and topography complicate modeling and data interpretation. Coolbaugh et al., (2007) specifically highlights the low thermal inertia and high albedo of sinter deposits, a result of the high porosity and bleached color of the deposit, respectively. These properties decrease in overall temperature during the day relative to surrounding rocks of similar composition, which causes sinter deposits like those present at Brady to appear as cool spots in thermal imagery, potentially masking signs of thermal anomalies and subsurface geothermal systems. These studies provide a critical baseline to test new method of remote thermal imaging, and are used as comparison and calibration to work presented here.

2.2 Technological Advancements and History

Improvements in imagery processing software, geographic information systems (GIS), global positioning systems (GPS), payload sensors, and data processing have increased the ability to process and analyze UAS survey data. Beginning in the 1950s, spatial analysis and aerial mapping required manned fixed-wing aerial flights to image the earth's surface from above. These photographs were often taken overlapping to be viewed as stereoscopic pairs (Birdseye, 1940; Howarth, 1996). Stereoscopic pairs use the eye's natural ability to view two photos from slightly different angle to project images into three-dimensional (3D) models. This process has continued to be used into the 21st century, especially by geoscientists and cartographers. Using the same principles of stereographic pairs, photogrammetry algorithms identify key features in multiple images to construct high-resolution gridded imagery mosaics (rasters) over large areas and are used to create digital surfaces in three dimensions (Schenk, 2005). Traditionally, imagery collected used in photomosaics require ground control points to be visible in acquired imagery to be geographically corrected. These ground control points are physical targets visible to the sky and measured by GPS, the measured coordinates are put into the software so final raster is georeferenced. Today, GPS are often incorporated into the camera, so that images include geographic location information, making this process more efficient. However, ground control points are still used to evaluate and increase accuracy in the final product.

Remote radio-controlled (RC) helicopters were first introduced in 1968, however it was not until the 1990's that these systems became more reliable and internationally popular, spurring development among government, industry, and academia. This was largely due to the inventions of light weight inertia measurement units (IMU) capable of measuring movement and direction of devices, which improve hover and control capabilities. Between 2005 and 2010, companies began producing hobby quad-copter UAS for consumers, which typically had flight battery lives of around three minutes. After 2010, a Chinese-based drone company, DJI, became the first company to vertically integrate all the technology, from hardware to software, controller to aircraft and payloads, needed to mass produce high-quality UAS for the public (Nonami, 2018). The DJI Phantom series was released in late 2012, ready to fly and easy to maneuver without engineering or extensive pilot experience. At that time the drone required manual mounting of camera equipment and flight times were limited to 10 minutes, but by setting a camera equipped with interval shutter periods and careful manual controls of flights in a pattern, it now became possible to collect on-demand imagery and incorporate photogrammetry stitching algorithms across industries and research institutions without fixed wing flights. The Phantom series upgrades through time included pre-mounted cameras, preprogrammed flight capabilities, and increased battery life on up to 45 minutes. This series remained popular until it was discontinued in 2023, replaced the increasing popular Mavic series.

Thermal cameras measure infrared radiation emitted from, through, or off of objects and software converts that value to temperature using an estimated or known emissivity index, ambient or reflected temperature, distance to object, and other environmental factors (Madding, 1999; Avdelidis and Moropoulou, 2022). Emissivity, the inverse of thermal reflectivity, is a measurement of how an object emits infrared radiation, a wavelength longer than visible light and associated with heat. Emissivity values are measured between zero and one, with one representing perfect black-body behavior. Lower emissivity materials incorporate more reflected or transmitted infrared radiation. Understanding and assessing emissivity is critical for interpreting thermal imagery. Objects with high emissivity can be reliably imaged and their temperatures can be interpreted from TIR images, while low emissivity objects incorporate more ambient, reflected radiation, and as a result their temperatures can be difficult or impossible to measure (Jin and Laing, 2006; Clausing, 2007). The angle of the camera or the geometry of the object also makes a difference in final temperatures calculation, with one study suggesting that an 80-degree camera angle (nearly perpendicular to the surface) is most optimal for accuracy of measurements (Lee and Lee, 2022). Ground control points with temperature readings can help in calibration and interpretation of collected thermal survey data (Maes et al., 2017).

Handheld thermal cameras are widely used in operating geothermal fields for manual inspection of electrical infrastructure, stationary emission inspection required by plant, and compliance reporting for leak detection. Thermal cameras were first introduced as an optional UAS payload on DJI's Matrice and Inspire Series in 2016. In 2018, the DJI Mavic 2 enterprise series included an TIR payload option, followed by the 2021 Autel Evo II Series (2021), and DJI's Mavic 3T (2022). These cameras continue to improve in resolution and accuracy with each new release (Fig. 2).

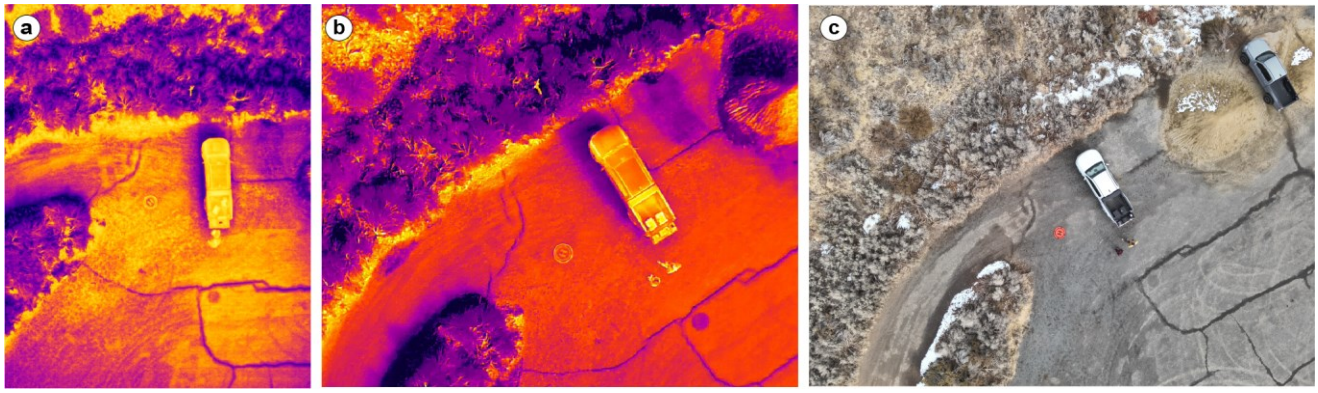

Figure 2: Thermal infrared imagery from single photos, take from a.) Autel Evo II version 2, released in June 2021, and b.) DJI Mavic 3T, released in September of 2022. Both models take TIR and RGB photos simultaneously, and wider angle of view is apparent in the c.) Mavic 3T RGB image. The Mavic images were taken at the same location and time via the dual camera payload. Notable features in these photos are heated ground on south facing surfaces (lower right), colder areas within pavement cracks, and relatively warmer persons in TIR images.

GIS software, designed to document, review, and analyze spatial data, allows users to digitally map on georeferenced (spatially-corrected, orthorectified) digital imagery. Digital enhancement of imagery is also available in GIS software applications, where layer blending and other digital optimization is useful in data analysis and interpretation of orthomosaics. Paired with the years of technologic advances described above, we can now create high-resolution, georeferenced imagery from UAS surveys, blended and digitally enhanced in spatial software, to improve in our spatial mapping and analysis efforts.

2.3 UAS Equipment and Federal Regulations

UAS, including quadcopters and fixed-wing aircraft, in the United States are regulated by the FAA. The FAA first released regulations covering drone operations in 2016, which have been refined into comprehensive set of rules and systems to support operations across the United States. Pilots flying for non-hobby purposes are required to obtain additional certifications under the Part 107 rule, which increases flexibility of operations and allows pilots to apply for waivers to certain aspects of the regulations (Truong et al.; 2024). Starting in 2021, the FAA have allowed for Part 107 certified pilots to fly their aircraft at night with enhanced lighting without obtaining a regulatory waiver to initiate these flights. This seemly small change has large impacts and implications for the geothermal industry. Night ambient temperatures are more stable and generally colder than daytime temperatures, and reduced solar radiation of surfaces improves visibility of thermal features in final digital products (Yang et al., 2024). By removing the need to acquire a waiver through the FAA, these flights can now be completed on shorter project planning windows and take advantage of favorable weather conditions as they arise.

Small UAS deployable under Part 107 rules must weigh under 55 pounds at takeoff, including any attached payloads. Even under that definition UAS are available in a variety of sizes, capabilities, and prices. Some of the smallest UAS weigh in at one-half to two pounds, have fixed payloads, and are thousands of dollars in price. FAA regulations limit flights to within line of sight, therefore typically these UAS have smaller ranges and coverage capabilities when compared to larger-sized UAS. Large UAS, eight to twenty pounds at takeoff, typically can support multiple interchangeable payload systems. These UAS can cost around tens of thousands of US dollars, not including payloads, which can be just as expensive. Large UAS are heavier and require more effort in planning and deploying flights, as well as increased power consumption and batteries.

Sensor factors to consider when selecting fit-for-purpose UAS are details including mechanical or digital shutters in camera drones, which can affect the amount of distortion in images from moving aircraft (İncekara and Seker, 2021). Country of origin is also a factor, as internationally manufactured UAS can be targets of restrictive legislation and customs acts. While UAS manufactured in the United States are becoming more available, DJI remains the dominant UAS supplier and technological innovator around the world (He et al., 2022). In an internal poll among Ormat's geoscience department, survey participants were asked about anticipated use, functionality factors (e.g. coverage, portability, shutter-type, software compatibility), price and country of origin importance of future UAS surveys. Low-cost, portable UAS with visible and thermal sensors, were identified as the most important in support of geothermal explorational and operational fieldwork.

3. DATA AND METHODS

3.1 Equipment & Flight Details

Ormat contracted a certified sUAS pilot to collect and process visible light and calibrated thermal imagery at Brady geothermal field in early 2024. Flights were completed between February 22nd-28th, 2024. Data were collected over multiple days and processed separately in four sections (Fig. 1). Final products included original photos from all cameras, processed thermal imagery, visible light and calibrated thermal orthomosaics, and digital surface models. Location and thermal ground control points and coverage area footprints were provided as GIS shapefiles. A total of 1.39 km^2 (340 acres), were targeted for daytime RGB surveys and night/predawn TIR flights. Ambient air temperatures during the night TIR flights averages ranged from -6.1 to -1.9 degrees Celsius.

Autel Robotic's Evo II Pro was used for daytime RGB flights. Front overlap of imagery was 78-82%, side overlap was 68-72%, with a total of 5,814 images processed into 1.4-1.7 cm/pixel orthomosaics, variable by processed sections. DJI's Mavic 3T was used for the TIR flights, which targeted midnight to sunrise flight times, with most flights between 2:00-7:00 am (Pacific Standard Time). A total of 15,567 images were processed into orthomosaics with a final resolution of 2-4.5 centimeter per pixel, again variable by processed sections. Temperature calculations during processing used a default emissivity value of 0.95, as set by the UAS manufacturer. Location and temperature control points, as well as ambient weather conditions, were used throughout the field area to calibrate and ground truth these data products. Final thermal raster values matched measured ground temperature within two to three degrees Celsius throughout the study area after calibration.

3.2 Post-processing and Spatial Analysis

In this study we utilize Environmental Systems Research Institute (ESRI) ArcPro and ArcGIS Enterprise software to view, analyze and share processed data across disciplinary teams. Post processing of the orthomosaics using ArcPro included spatial analysis and symbology configuration, where the Inferno (yellow-to-purple) color bar was applied to the TIR raster with the stretch option enabled across negative five to positive eight degrees Celsius (Fig. 3). To further aid visual inspection and mapping, a graphical Lightening layer blend was applied to enhance and combine the TIR and RGB raster layers. The Lightening blend is digital image editing schema that compares data from each raster layer and retains the lighter color in the final image, creating a glow around the areas of hot ground (bright on the colormap) but allowing viewer to still view RGB imagery in areas of cooler ground.

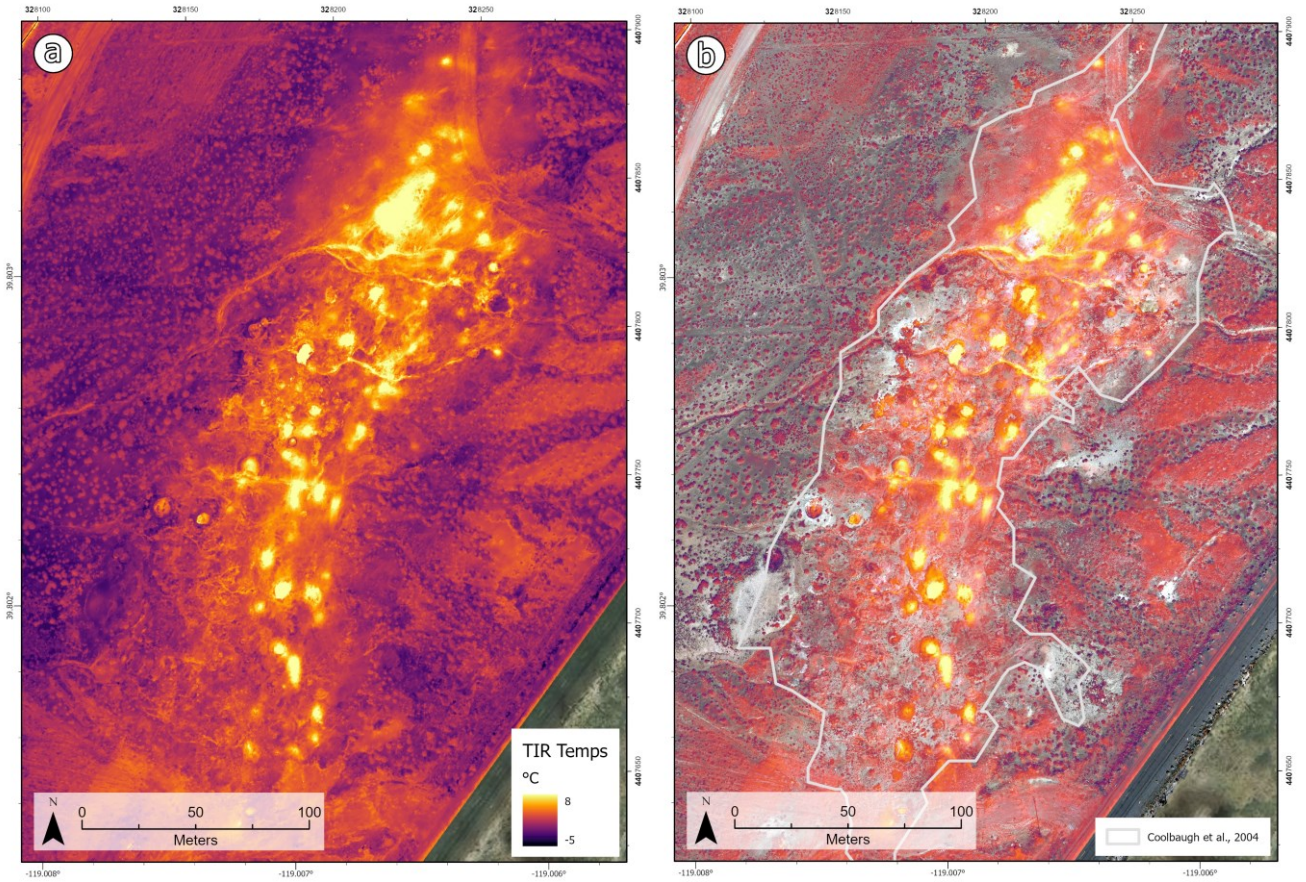

Figure 3. TIR imagery of heated ground in the northern portion of the Brady geothermal field. a.) Raster is symbolized in Inferno color ramp stretched between -5 and 8 degrees Celsius. b.) A digital lightening affect applied to merge TIR and RGB imagery and overlain by Coolbaugh et al.'s (2004) warm ground polygon.

The imagery was visually inspected to determine a contour interval that would most clearly define areas of anomalous heat, with two-degree Celsius intervals mostly closely resembling Coolbaugh et al. (2004) work and five-degree intervals clearly defining the hottest areas (Fig. 4). Contours and polygon features were extracted in order to calculate area of heated ground. This method combines high-resolution analytical power of GIS with visual confirmation and user input to obtain a robust analytical measurement of heated areas. Environmental changes, like ambient air temperatures, affect the physical temperature reading that makes no two surveys fully repeatable. However, the increased resolution and coverage using the UAS TIR method presented here is still much improved from handheld instrumentation and GPS mapping of heated ground and vents alone. This method is especially useful in areas like Brady where heated and steaming ground dominate the landscape without measurable spring discharge locations.

Spatial data products were published to an ArcGIS Enterprise dashboard to increase visibility and sharing across Ormat departments. The Enterprise system is internally hosted software installed on internal servers for increase data security. Software dashboards are generally map-based, but can include tables, photos, and file attachments to assist users in quick viewing of data without needing to download data or be physically involved in acquisitions.

4. RESULTS AND DISCUSSION

The UAS TIR revealed elevated heated ground thermal manifestations and anomalously heated ground over a dispersed area primarily focused within the stepover in the northern study area and along a northeast trend in the southern study area (Figs. 1, 4). The anomalously heated ground measuring greater than two-degrees Celsius in the northern area of the study overlaps 19,764.7 of the 24,240.2 square meters mapped by Coolbaugh et al. (2004) shown in the orange polygon in figure 4a. Using a similar method, the southern area of the study footprint has an area of anomalously heated ground of 12,288.4 square meters while the previous study measures 10,467.5 square meters (Fig. 4b). In both locations, mapped areas from this study have similar size and shape to that identified by the previous study, within a 17-18% change. The correlation between the UAS TIR imagery and the mapped thermal anomaly supports that the UAS method is accurate and provides high resolution data. It is unknown if minor changes in the size and shape of the thermal anomaly are due to the increased accuracy of UAS surveys, changes in heated ground distribution at the field over time, or difficulty in repeating these types of measurements due to environmental conditions, like weather and climate fluctuations. Areas of mapped silicified deposits correlated with cold spots in the TIR imagery, as highlighted in previous work (Coolbaugh et al., 2007). While Coolbaugh et al. (2007) recognized this cooler ground as a potential mask to subsurface thermal anomalies, these data may be utilized to further improve mapping and identification of mineralization at geothermal fields.

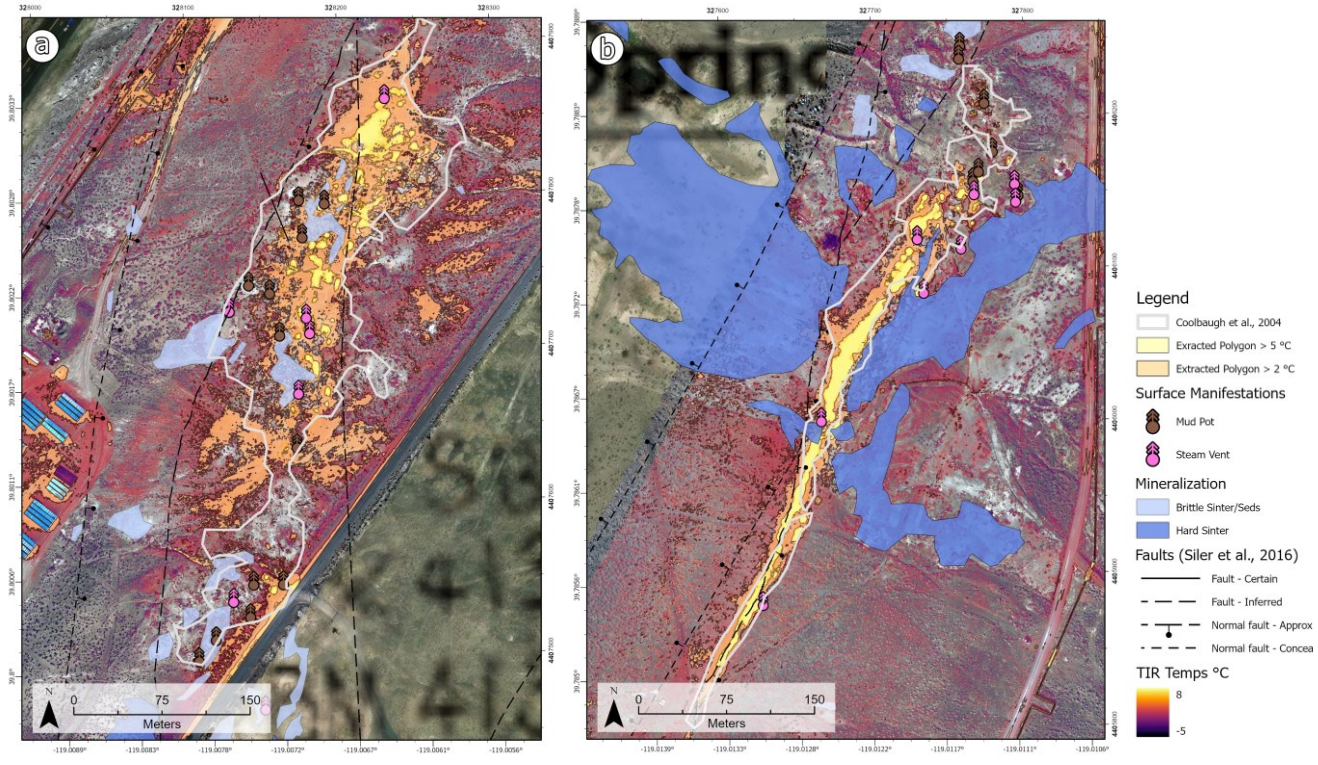

Figure 4. RGB and TIR orthomosaics, with Lightening digital blend applied shown in base map, GIS extracted polygons of heated areas greater than two- and five-degree Celsius, geologic surface manifestations and mineralization, and Coolbaugh et al. (2004) outline of warm ground overlain. Northern area of disperse heat shown in figure a, and southern area in figure b.

The imagery captured here is also useful in monitoring infrastructure across the operating field. The thermal imagery successfully recorded heat anomalies along production wellheads, uninsulated and buried pipelines (Figs. 5, 6). However, low emissivity values (0.2-0.5) of metallic surfaces, including infrastructure or equipment, make direct temperature measurements difficult. While these reflective surfaces look relatively cool in the TIR imagery, temperature anomalies along these features are still visible in orthomosaics, as the processed TIR values of surrounding heated ground more closely represent the true temperatures (i.e. have surface emissivity values close to the 0.95 used in imagery processing).

Heated features identified in TIR images were reviewed in RGB imagery prior to field checks and confirmed that the areas of hottest infrastructure shown in figure 5a and 6a were the results of missing insulation, which had been recently removed to complete maintenance work. In figure 6, pipeline buried under a dirt road in the southern part of the field, is also visible in the TIR imagery. Heat from electrical transformers used in powering downhole production pumps are visible from the TIR images shown in figure 5b. These observations demonstrate that TIR UAS can be used to help optimize the efficiency of the plant by identifying and reducing heat or fluid losses, both

above and below ground, without disturbing ground or putting anyone in the proximity of heated areas or infrastructure. The full utility of UAS for safety and infrastructure monitoring will continue to be assessed by Ormat as the technology advances.

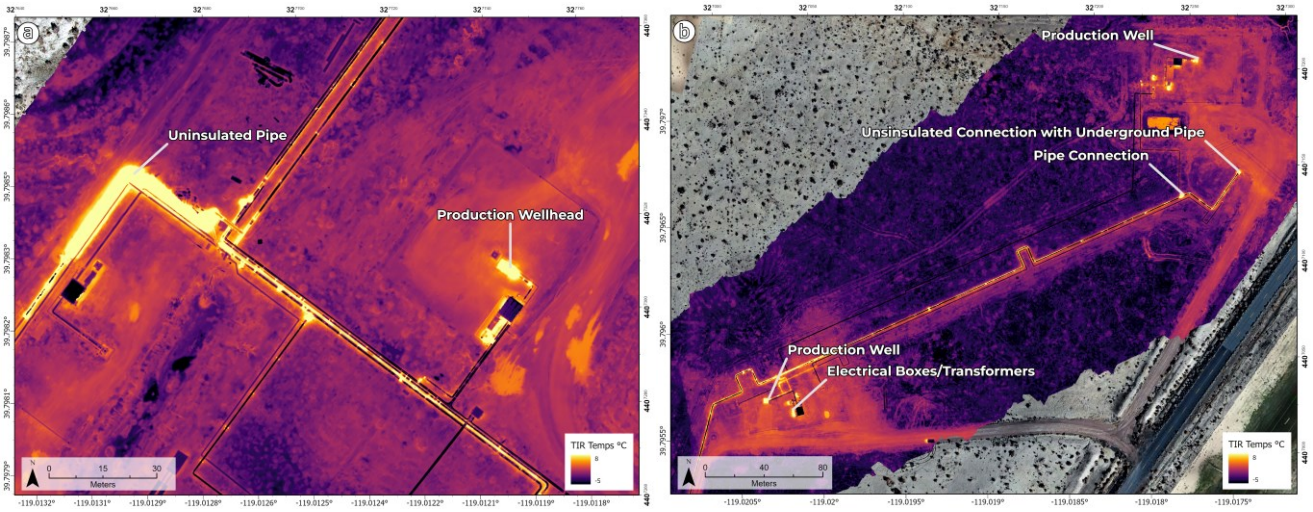

Figure 5: TIR imagery of operation infrastructure at Brady field, highlighting heated area around uninsulated brine pipeline, location of production wellheads, cellars (a,b), as well as pipe connections and electrical boxes (b).

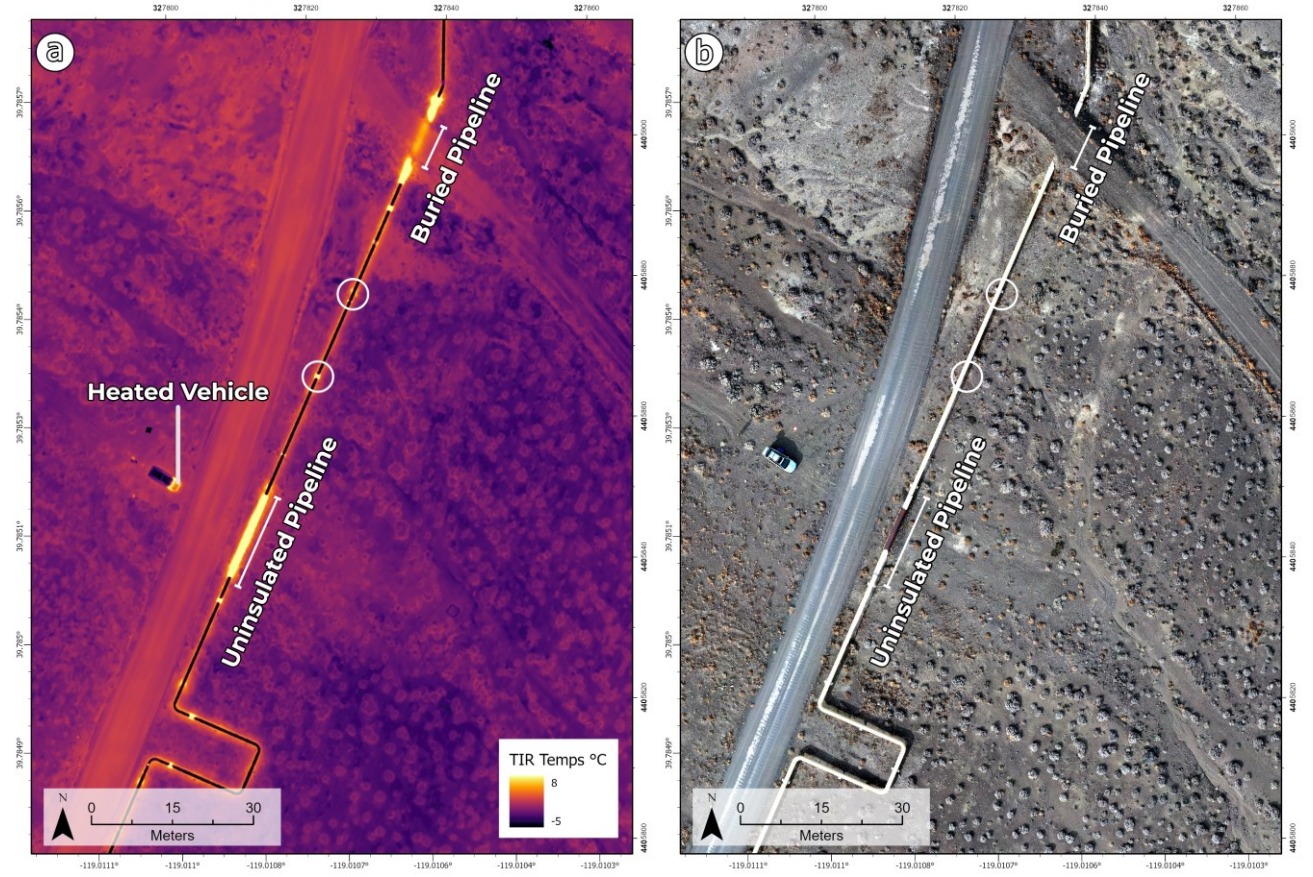

Figure 6. Survey imagery collected along the injection pipeline south of the Brady power plant, showing ability of (left) TIR imagery to identify uninsulated and buried pipeline, confirmed in (right) RBH imagery and field inspections. Circles show location of pipe stands and reduced insulation.

5. CONCLUSION

In this study, we show how data collection using TIR and RGB sensors have the potential to improve our understanding of geothermal systems and help optimize geothermal operations. Geologic analysis of geothermal systems is significantly bolstered using TIR and RGB imagery by identification of thermally heated areas and surface manifestations at higher resolution and greater efficiency than previously possible. Thermal UAS may also be used to increase resolution of mapped mineralization and sinter deposits by better identifying relatively colder areas in TIR imagery, as paired with ground truthing. These observations are both visually helpful and quantifiable by temperature and area calculations. Previous methods used to map thermal features in detail included walking the extent of surface manifestations, heated ground, and mineralized areas. Studies using these methods alone risk overlooking important features, are time consuming and potentially hazardous. In tandem with traditional ground-based methods, thermal UAS surveys can aid in focusing field efforts and decrease the risk of overlooking a zone of alteration or thermal manifestations, while keeping fieldworkers safe distance. Future surveys may shed light further on changes in the distribution of heated ground through annual cycles, climatic changes, or operational influence. Additional future work may include coupling UAS TIR imagery with two-meter temperature surveys for a more robust understanding of UAS TIR temperature sensitivities and depth-of-investigation capabilities.

At operational fields, we've shown how UAS can be used to survey geothermal infrastructure, which may lead to identification of, and assist in the remediations of, issues or inefficiencies of the system. These surveys have the potential to improve efficiency and effectiveness of work, but also significantly increase safety by identifying hazards associated with heated ground and equipment at our geothermal fields prior to entering dangerous situations. UAS surveys can reduce risk of injury, or even loss of life, by ensuring employees are fully aware and prepared for challenges present in their workplace prior to exposure. This method would not be possible without the work across many industries and advancements of technologies available today. Changes in regulations, like improved ability to conduct operations beyond visual line of sight may improve security, monitoring, emergency response, and technical evaluations of geothermal fields into the future. Continued improvements in GIS systems, sensors and payloads will only improve this process of data collection and sharing across the geothermal industry.

ACKNOWLEDGEMENTS

The authors thank Ormat Technologies, Inc. for permission to publish this work, in particular those who supported this work and future UAS deployments Adrian Wiggins, Peter Jahl, Aubry Burgess, and Richard Morrison. Thanks also to Owen Callahan at En Échelon Geosolutions for delivering high-quality calibrated data and supporting our team with technical knowledge and insights during this study.

REFERENCES

Angster, S., Wesnousky, S., Huang, W. L., Kent, G., Nakata, T., & Goto, H. (2016): Application of UAV photography to refining the slip rate on the Pyramid Lake fault zone, Nevada. Bulletin of the Seismological Society of America, 106(2), 785-798.

Aminifar, F. and Rahmatian, F., (2020): Unmanned aerial vehicles in modern power systems: Technologies, use cases, outlooks, and challenges. IEEE Electrification Magazine, 8(4), pp.107-116.

Avdelidis, N. P., & Moropoulou, A. (2003): Emissivity considerations in building thermography. Energy and Buildings, 35(7), 663-667.

Benoit, W. R., & Butler, R. W. (1983): A review of high-temperature geothermal developments in the northern Basin and Range province. Geotherm Resource Council Spec Rep, 13, 57-80.

Birdseye, C. H. (1940): Stereoscopic phototopographic mapping. Annals of the Association of American Geographers, 30(1), 1-24.

Bjornsson, G., Grimsson, G., Sigurdsson, A., & Laenen, V. S. (2019): Thermal mapping of Icelandic geothermal surface manifestations with a drone. In Proceedings of 44th Workshop on Geothermal Reservoir Engineering (pp. 1-8).

Burdziakowski, P., & Bobkowska, K. (2021): UAV photogrammetry under poor lighting conditions—Accuracy considerations. Sensors, 21(10), 3531.

Callahan, O. (2023): High-resolution structure-from-motion models of hydrothermal sites in the Central Nevada Seismic Belt: applications in tectonic, climate, and hydrothermal investigations. In Proceedings 48th Workshop on Geothermal Reservoir Engineering, Stanford University, Stanford, California.

Calvin, W. M., Littlefield, E. F., & Kratt, C. (2015). Remote sensing of geothermal-related minerals for resource exploration in Nevada. Geothermics, 53, 517-526.

Carrivick, J. L., Smith, M. W., & Quincey, D. J. (2016): Structure from Motion in the Geosciences. John Wiley & Sons.

Chio, S. H., & Lin, C. H. (2017): Preliminary study of UAS equipped with thermal camera for volcanic geothermal monitoring in Taiwan. Sensors, 17(7), 1649.

Clausing, L. T. (2007): Emissivity: Understanding the difference between apparent and actual infrared temperatures. Fluke Application Note, Fluke Education Partnership Program, www. fluke. com.

Coolbaugh, M. F., Kratt, C., Fallacaro, A., Calvin, W. M., & Taranik, J. V. (2007). Detection of geothermal anomalies using advanced spaceborne thermal emission and reflection radiometer (ASTER) thermal infrared images at Bradys Hot Springs, Nevada, USA. Remote Sensing of Environment, 106(3), 350-359.

Coolbaugh, M.F., Sladek, C., and Kratt, C. (2004): Digital mapping of structurally controlled geothermal features with GPS units and pocket computers. Geothermal Resources Council Transactions, 28, 321-325.

Gheisari, M., & Esmaeili, B. (2016): Unmanned aerial systems (UAS) for construction safety applications. In Construction Research Congress 2016 (pp. 2642-2650).

Faulds, J.E., Coolbaugh, M.F., Vice, G.S., & Edwards, M.L. (2006): Characterizing structural controls of geothermal fields in the Northwestern Great Basin: A Progress Report. Geothermal Resources Council Transactions, 30, 69-76.

Faulds, J. E., Moeck, I., Drakos, P., & Zemach, E. (2010a): Structural assessment and 3D geological modeling of the Brady's geothermal area, Churchill County (Nevada, USA): a preliminary report. In Proceedings, thirty-fifth workshop on geothermal reservoir engineering, Stanford: Stanford University.

Faulds, J. E., Coolbaugh, M. F., Benoit, D., Oppliger, G., Perkins, M., Moeck, I., & Drakos, P. (2010b). Structural controls of geothermal activity in the northern Hot Springs Mountains, western Nevada: The tale of three geothermal systems (Brady's, Desert Peak, and Desert Queen). Geothermal Resources Council Transactions, 34, 675-683.

Folsom, M., Lopeman, J., Perkin, D., & Sophy, M. (2018, February). Imaging shallow outflow alteration to locate productive faults in Ormat's Brady's and Desert Peak fields Using CSAMT. In Proceedings of the 43rd Workshop on Geothermal Reservoir Engineering, Stanford, CA, USA (pp. 12-14).

Harvey, M. C., Rowland, J. V., & Luketina, K. M. (2016). Drone with thermal infrared camera provides high resolution georeferenced imagery of the Waikite geothermal area, New Zealand. Journal of Volcanology and Geothermal Research, 325, 61-69.

He, X., Li, J., & Zhu, R. (2022): The Study of Company Competitive Strategy under new Manufacturing Industry-Taking DJI as an Example.

Howarth, R. J. (1996): History of the stereographic projection and its early use in geology. Terra Nova, 8(6), 499-513.

Hubbard, S., Pak, A., Gu, Y., & Jin, Y. (2017). UAS to support airport safety and operations: Opportunities and challenges. Journal of unmanned vehicle systems, 6(1), 1-17.

İncekara, A. H., & Seker, D. Z. (2021): Rolling shutter effect on the accuracy of photogrammetric product produced by low-cost UAV. International Journal of Environment and Geoinformatics, 8(4), 549-553.

Jin, M., & Liang, S. (2006): An improved land surface emissivity parameter for land surface models using global remote sensing observations. Journal of Climate, 19(12), 2867-2881.

Jiménez-Jiménez, S. I., Ojeda-Bustamante, W., Marcial-Pablo, M. D. J., & Enciso, J. (2021): Digital terrain models generated with low-cost UAV photogrammetry: Methodology and accuracy. ISPRS International Journal of Geo-Information, 10(5), 285.

Lai, C. J., Liu, J. K., Hsu, W. C., Li, K. S., Wu, M. C., & Chang, K. T. (2018): An experiment of geothermal exploration with an UAS-TIR in Xiaoyoukeng area of Tatun volcanoes, Taiwan. In IGARSS 2018-2018 IEEE International Geoscience and Remote Sensing Symposium (pp. 7882-7885). IEEE.

Laboso R, K & Davatzes, N., (2016): Fault-Controlled Damage and Permeability at the Brady Geothermal System, Nevada, USA. In Proceedings 41st Workshop on Geothermal Reservoir Engineering, Stanford University, Stanford, California.

Lee, K., & Lee, W. H. (2022): Temperature accuracy analysis by land cover according to the angle of the thermal infrared imaging camera for unmanned aerial vehicles. ISPRS International Journal of Geo-Information, 11(3), 204.

Li, X., Xiong, B., Yuan, Z., He, K., Liu, X., Liu, Z., & Shen, Z. (2021): Evaluating the potentiality of using control-free images from a mini Unmanned Aerial Vehicle (UAV) and Structure-from-Motion (SfM) photogrammetry to measure paleoseismic offsets. International Journal of Remote Sensing, 42(7), 2417-2439.

Madding, R. P. (1999): Emissivity measurement and temperature correction accuracy considerations. In Thermosense XXI (Vol. 3700, pp. 393-401). SPIE.

Maes, W. H., Huete, A. R., & Steppe, K. (2017): Optimizing the processing of UAV-based thermal imagery. Remote Sensing, 9(5), 476.

Maset, E., Fusiello, A., Crosilla, F., Toldo, R., & Zorzetto, D. (2017): Photogrammetric 3D building reconstruction from thermal images. ISPRS Annals of the Photogrammetry, Remote Sensing and Spatial Information Sciences, 4, 25-32.

McGuire, M., Rys, M. J., & Rys, A. (2016): A study of how unmanned aircraft systems can support the Kansas Department of Transportation's efforts to improve efficiency, safety, and cost reduction.

Nishar A, Richards S, Breen D, Robertson J, Breen B. (2016): Thermal infrared imaging of geothermal environments and by an unmanned aerial vehicle (UAV): A case study of the Wairakei–Tauhara geothermal field, Taupo, New Zealand. Renewable Energy. 86:1256-64.

Nonami, K. (2018): Research and development of drone and roadmap to evolution. Journal of Robotics and Mechatronics, 30(3), 322-336.

Rymer, N., & Moore, A. J. (2021): A Review of Unmanned Aerial Vehicle Technology in Power Line Inspection. AIAA Scitech 2021.

Schenk, T. (2005): Introduction to photogrammetry. The Ohio State University, Columbus, 106(1), 1.

Siler, D.L., Hinz, N.H., Faulds, J.E., & Queen, J.H. (2016): 3D analysis of geothermal fluid flow favorability: Brady's, Nevada, USA. In Proceedings 41st Workshop on Geothermal Reservoir Engineering, Stanford University, Stanford, California.

Siler, D. L., Faulds, J. E., Hinz, N. H., & Queen, J. H. (2021): Three-dimensional geologic map of the Brady geothermal area, Nevada (No. 3469). US Geological Survey.

Truong, D., Lee, S. A., & Nguyen, T. (2024): How to Enhance Safety of Small Unmanned Aircraft Systems Operations in National Airspace Systems. Drones, 8(12), 774.

Remondino, F., Barazzetti, L., Nex, F. C., Scaioni, M., & Sarazzi, D. (2011): UAV photogrammetry for mapping and 3D modeling: Current status and future perspectives. In Proceedings of the International Conference on Unmanned Aerial Vehicle in Geomatics (UAV-g): 14-16 September 2011, Zurich, Switzerland (pp. 25-31). International Society for Photogrammetry and Remote Sensing (ISPRS).

Wesnousky, S. G., Barron, A. D., Briggs, R. W., Caskey, S. J., Kumar, S., & Owen, L. (2005). Paleoseismic transect across the northern Great Basin. Journal of Geophysical Research: Solid Earth, 110(B5).

Wright, W. D. (1954): Stereoscopic vision applied to photogrammetry. The Photogrammetric Record, 1(3), 29-49.

Yang, B., Wang, D., & Zhang, R. (2024). Methods to mitigate the impact of work environment on the measurement of building surface temperature by unmanned aerial vehicle onboard thermal imaging system. Energy and Buildings, 324, 114872.

Yeom, S. (2024): Thermal Image Tracking for Search and Rescue Missions with a Drone. Drones, 8(2), 53.